Diurnal Coastal-Trapped Waves on the East Australian Continental Shelf

HOWARD J. FREELAND

Institute of Ocean Sciences, Sidney, B.C., Canada

10 August 1987 and 2 November 1987

ABSTRACT

Data obtained during the Australian Coastal Experiment, previously used to verify the dispersion relation for coastal-trapped waves at low frequencies, are analyzed at frequencies in the diurnal tidal band. It is shown that only a single (the first) mode is required to describe the cross shelf and slope distribution of alongshore currents in contrast to the low frequency limit where at least two and arguably three modes were needed. Furthermore, it is shown that the alongshore structure of these modes yields a good fit to the dispersion relation and its slope in the ω–k plane.

1. Introduction

In a recent series of papers, Freeland et al. (1986) and Church et al. (1986a,b) examined the propagation of coastal-trapped waves (hereinafter, CTWs) at low frequencies ($\omega/f \ll 1$). The data analyzed were obtained as part of the international Australian Coastal Experiment (ACE) that took place between September 1983 and March 1984. Figure 1 shows a map of the south eastern part of Australia locating the five mooring lines deployed in ACE and, specifically, the three principal lines on which the analysis of this paper will be based. ACE permitted a detailed examination of the dynamics of flow on the east Australian continental shelf and slope, and in particular a description of the propagation and structure of low frequency CTW modes propagating within the coastal waveguide. Essentially the above papers verified that the fluctuating currents satisfied the modal structures and dispersion relations of low frequency CTWs. The cited papers examined fluctuations at periods $24 \geq T \geq 4$ days, mainly because large signals were evident in this range that corresponds to the range of strong weather forcing. However, substantial energy also exists at diurnal tidal periods. Furthermore, at the latitudes of ACE the inertial period is 19.7, 21.1 and 21.7 h at mooring lines 1, 2 and 3, respectively, (see Fig. 1) and so there is no obvious obstacle to the propagation of CTWs at diurnal periods. Coastal-trapped waves at diurnal periods have been observed elsewhere: off the coast of Vancouver Island, see Thomson and Crawford (1982) and Crawford and Thomson (1984); in the Weddell Sea, Middleton et al. (1987); and off Sakhalin Island, Yefimov and Rabinovich (1980). The purpose of this paper is to examine the structure of the current field at the K_1 and O_1 tidal lines and verify that these current fluctuations also satisfy the modal structure and dispersion characteristics appropriate to CTWs.

The remainder of this note is organized as follows. In section 2 the modal structure of the tidal currents is analyzed at each of the three principal lines of current meter moorings. In section 3 the results are interpreted in terms of a wave fit and the fit is compared with the theoretical dispersion relations for CTWs.

2. On–offshore structure of alongshore currents

For each current meter location an harmonic analysis was performed using the scheme developed by Foreman (1978) to obtain the amplitude and phase of the alongshore component of current at the two principal diurnal tidal lines K_1 and O_1. The time series for the most part were long enough (>6 months) that the P_1 constituent could be computed and so does not contaminate K_1.

A detailed examination of harmonic constituents shows a strong tendency for the currents at K_1 and O_1 to have the same Greenwich phase. This in turn suggests that the cross-shore distribution of alongshore currents is controlled by some form of cross-shore modal structure, possibly that of coastally trapped waves.

Using the same Brunt–Väisälä frequency and depth distributions as were used in the Freeland et al. (1986) and Church et al. (1986a,b) papers the CTW dispersion relations were computed for general frequency distributions. The shape of the first CTW mode at each of the three principal mooring lines is plotted on Figs. 2a–c. The modal shape is computed at a frequency intermediate between the K_1 and O_1 tidal frequencies using a program kindly supplied by Dr. K. Brink. The

Corresponding author address: Dr. Howard J. Freeland, Institute of Ocean Sciences, P.O. Box 6000, Sidney, British Columbia, Canada V8L 4B2.

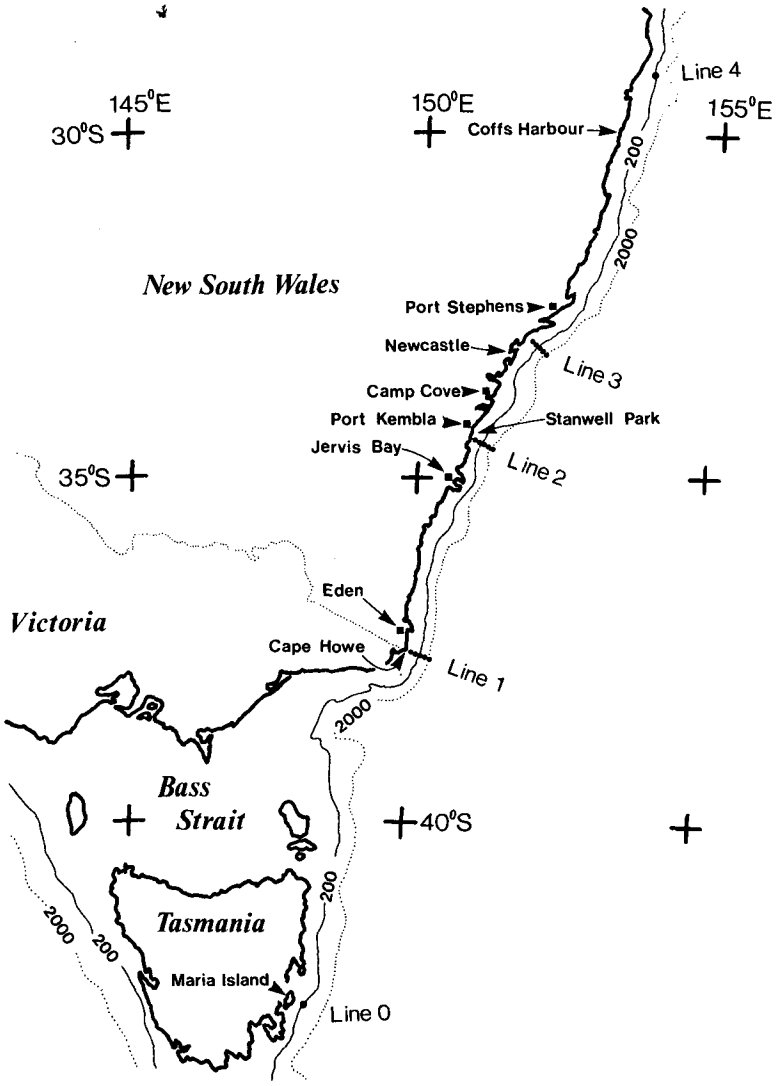

FIG. 1. Map of southeastern Australia showing the general area of the Australian Coastal Experiment. Current meter locations are marked by the symbol ●, and the three principal lines of moorings used in this paper are indicated as lines 1, 2 and 3.

programs used (BIGLOAD2 and CROSS) are described and documented by Brink and Chapman, 1985. It is entirely arbitrary how the modal shapes and, consequently, the amplitudes of the modes are normalized. The product of the modal distribution and its amplitude must, however, yield a velocity in some appropriate units. In all of the following, the modal shapes are assumed to be dimensionless and are normalized to have a unit amplitude at the shallowest current meter on the near-shore mooring. The amplitudes are dimensionally correct to represent a near-shore current speed in mm s^{-1}.

The modal shapes shown in Figs. 2a–c are different from the low-frequency modes used in the earlier ACE papers though obvious similarities do exist. These modes have a somewhat larger dynamic range, and the zero contour is shallower than in the low-frequency case. These details are unimportant, what is important is that a modal description different from that used in the earlier papers must be used. The second modes were also computed, but these are not presented here. In the high frequency case the first mode phase speeds range from 3.17 (line 1) to 3.87 m s^{-1} (line 3). This is a much smaller range than that found in the low frequency limit of 3.20 (line 1) to 5.15 m s^{-1} (line 3).

Consider one line of moorings, we compute an amplitude d_i and Greenwich phase g_i for the current meter location number i along that line. For simplicity let us represent that amplitude/phase as a complex number $\hat{d}_i$ and let us represent that observation as the superposition of two modes M_1 and M_2 evaluated at location i, i.e.

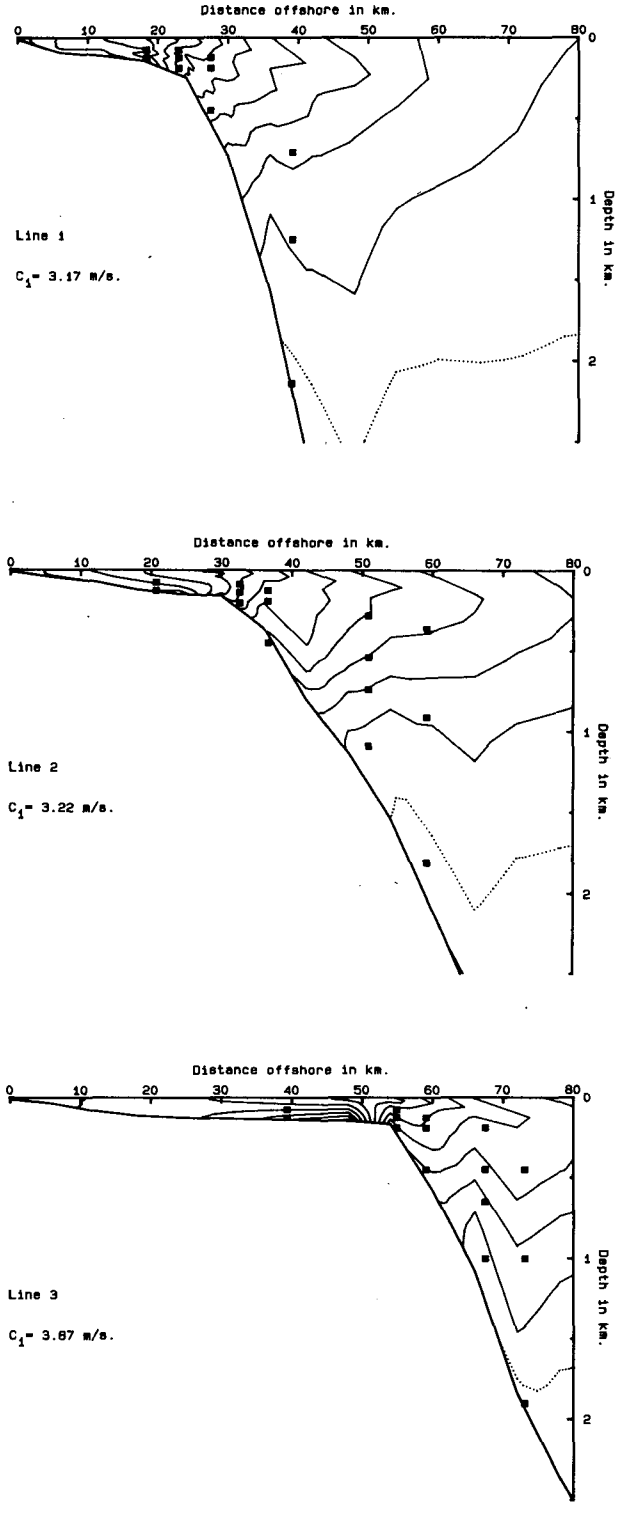

FIG. 2. Contour plot showing the shape of the first CTW mode and associated phase speed (C_1) along each of the three principal lines of moorings in ACE. The solid squares indicate the locations of current meters used in the analysis of this paper. The dotted line indicates a zero contour. The modes are normalized so that each has unit magnitude at the shallowest current meter (75 m) on the closest mooring to shore, and the contour interval is 0.1 (nondimensional).

$$\text{best fit } (\hat{d}_i) = \hat{a}_1 M_{1i} + \hat{a}_2 M_{2i}. \tag{1}$$

We define an error measure as

$$\hat{E}_i = \hat{d}_i - \hat{a}_1 M_{1i} - \hat{a}_2 M_{2i} \tag{2}$$

and an error norm for the whole line as

$$E = \sum_{i=1}^{N} \hat{E}_i^* \hat{E}_i. \tag{3}$$

In all of the above the carat symbol denotes a complex number and the asterisk a complex conjugate. Minimizing E in (3) yields the best fit modal amplitudes. The oceanic Kelvin wave has a large on–offshore length scale determined by the Rossby radius of deformation $R = \sqrt{gH}/f$ where H is an abyssal ocean depth. For a Kelvin wave we expect the alongshore component of velocity to be in geostrophic balance with the cross-shore pressure gradient. Thus $fv = -g\partial h/\partial x$ where $h \approx h_0 \sin(\omega t) \exp(-x/R)$ is the fluctuating part of sea surface elevation at frequency ω. Hence, $v \approx v_0 \sin(\omega t) \times \exp(-x/R)$ where $v_0 \approx h_0\sqrt{g/H}$. Fandry et al. (1985) give a typical K_1 tidal amplitude, h_0, of about 15 cm in the southern ACE region and off the New South Wales coast the abyssal depth is around H = 4900 m. Thus we expect typical alongshore velocities associated with the Kelvin wave to be around 0.7 cm s^{-1} if all of the signal is due to a Kelvin wave. In the following analysis we will neglect any contribution from the oceanic Kelvin wave. The velocity signal due to the Kelvin wave is expected to be small and was observed to be small in Crawford and Thomson (1984).

Table 1 shows the results of fitting modes in the least-squares sense to observations at K_1 and O_1 tidal lines, and to mooring lines 1, 2 and 3. For each mooring line we list the results of two fits; the first involves fitting mode 1 alone and the second a fit of the first and second

TABLE 1. Best fit amplitudes (in mm s^{-1}) and phases for modes 1 and 2 computed singly or simultaneously at lines 1, 2 and 3, and at O_1 and K_1 tidal lines.

Line	a_1	ϕ_1	a_2	ϕ_2	ϵ
			K_1		
1	56.4	301.6	—	—	0.137
	56.7	302.2	1.2	183.6	0.137
2	28.8	55.6	—	—	0.312
	22.4	34.0	16.1	101.5	0.210
3	41.0	319.7	—	—	0.283
	41.9	319.5	3.5	128.8	0.276
			O_1		
1	27.0	262.6	—	—	0.154
	24.8	271.6	9.0	205.3	0.129
2	20.9	336.0	—	—	0.179
	20.0	323.2	6.5	49.0	0.141
3	13.8	236.2	—	—	0.656
	13.0	240.4	4.9	187.2	0.597

modes simultaneously, as in equations (1), (2) and (3). The amplitudes listed in Table 1 are defined as $a_1 = |\hat{a}_1|$, and listed in mm s^{-1}, and the phases $\phi_1 = \arctan[I_m(\hat{a}_1)/\mathrm{Re}(\hat{a}_1)]$. The final column lists the residual variance as a fraction of the total variance, i.e.

$$\epsilon = E/\sum_{i=1}^{N} \hat{d}_i^* \hat{d}_i.$$

For a perfect fit ϵ would be zero. In all but one case (O_1, mooring line 3) the fit to mode 1 alone is efficient, accounting for 69% to 86% of the variance. In the one poor fit only 35% of the variance is accounted for by the mode-1 fit. In all cases the improvement in fit that results from including the second mode is very small, and in the rest of this paper we will use the results from the mode-1 fit alone.

3. Phase propagation

The interpretation of the phases in Table 1 leads to some minor difficulties. At the expected phase speed of around 3.5 m s^{-1} we expect a diurnal wave to have a wavelength of around 300 km. However, the alongshore distance between lines 1 and 2 is 360 km, and that between lines 2 and 3 is 160 km. Hence we expect a phase difference between lines 1 and 2 of somewhat more than 360°. Figure 3 presents a plot of the phases derived from those listed in Table 1. The phases for line 3 are plotted exactly as listed; for line 2 the K_1 phase is plotted as listed, for O_1 the listed phase of 336° is plotted as −24°; for line 1 the phases are changed by subtracting twice 360°. Other plausible phase distributions can be found by adding or subtracting various multiples of 360°, but if we fit a regression line through the plotted phases this distribution produces the line with least residual error. Hence in an objective sense if we expect a linear phase propagation then this arrangement is the most plausible arrangement.

It is evident from Fig. 3 that a linear phase propagation rate fits fairly well. The solid line indicates a best fit through the six phase observations of a slope of 1.34° km^{-1}, or a wave length of 268 km. Also evident in Fig. 3 is the steady divergence of O_1 and K_1 phases with increasing distance northward. Figure 4 shows a plot of K_1 minus O_1 phase versus alongshore distance. The regression slope is proportional to the difference in wavenumber between K_1 and O_1 frequencies.

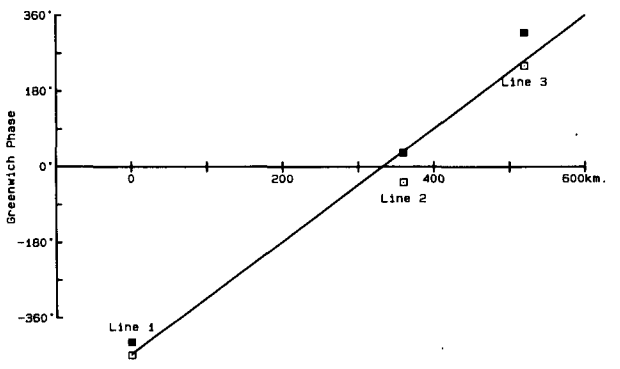

FIG. 3. Greenwich phase of mode 1 at K_1 and O_1 tidal lines (solid and open squares respectively) plotted against distance alongshore. The solid line is a regression line fitted through these phase estimates.

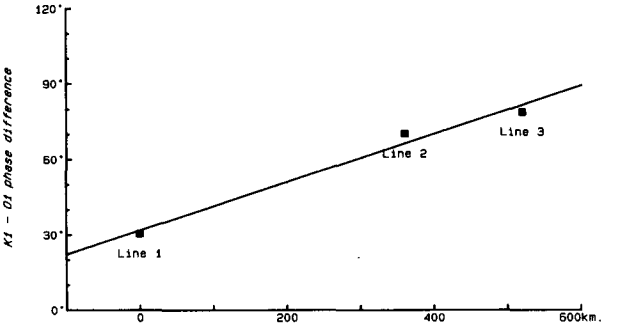

FIG. 4. The difference in phase between K_1 and O_1 tidal lines plotted against distance alongshore.

Figure 5 shows a plot of the complete dispersion relations for the mode-1 CTW between zero frequency and the high frequency cutoff at f for each of the three mooring lines. The small squares near the origin show the wavenumber/frequency relations estimated by Freeland et al. (1986) for mode 1 at low frequencies. The dotted box shows the region of the ω–k plane examined previously by Freeland et al. The O_1 and K_1 frequencies are indicated. At the frequency intermediate between O_1 and K_1 we enter a square symbol

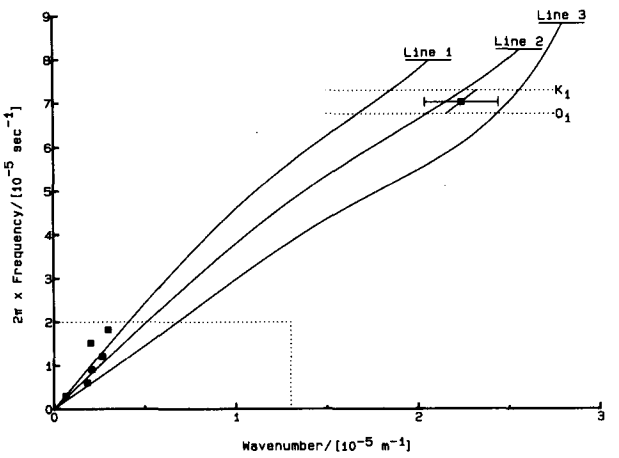

FIG. 5. The dispersion relation for mode 1 CTWs in ACE. The solid squares at lower left indicate estimates from previous analysis of the low frequency limit. The solid lines indicate the theoretical dispersion relations expected at the three principal lines of moorings in ACE. The single solid square between K_1 and O_1 frequencies indicates a single estimate of the dispersion relation based on the present analysis. The error bars indicate 95% confidence limits, and the short sloping line indicates the local value of $d\omega/dk$ estimated from Fig. 4.

indicating the wavenumber estimated from the slope in Fig. 3. The error bars shown are 95% confidence intervals. The sloping line through the box indicates the difference in wavenumber expected between O_1 and K_1 frequencies, based on the regression line of Fig. 4, i.e. the local slope of the dispersion curve.

4. Conclusions

An analysis of the ACE dataset in the diurnal tidal band indicates that the current field is fitted well by a single coastal-trapped wave mode. The alongshore phase variation of this mode indicates linear phase propagation and an excellent fit to the theoretical dispersion relations. Finally, the variation of phase across the diurnal band yields an estimate of the local slope of the dispersion curve which fits the expected slope accurately.

A previous paper verified the dispersion curves at low frequencies; we now conclude that the dynamics of coastal-trapped waves is also verified at high frequencies near the limit imposed by the local Coriolis parameter.

Given that the local inertial period is less than the periods associated with the diurnal tidal band this is perhaps not surprising. What would be very interesting, however, would be to look at the structure of the diurnal tidal waves as they pass a little farther to the north where the K_1 and O_1 lines approach and then cross the local inertial period. This point is achieved between lines 3 and 4, see Fig. 1. Presumably north of this "turning latitude" where $\omega = f$ the coastal-trapped waves can still propagate, but only as leaky evanescent modes. This possibility is being investigated.

REFERENCES

Brink, K. H., and D. C. Chapman, 1985: Programs for computing properties of coastal-trapped waves and wind-driven motions over the continental shelf and slope. Woods Hole Oceanogr. Inst. Tech. Rept., WHOI-85-17.

Church, J. A., H. J. Freeland and R. L. Smith, 1986a: Coastal-trapped waves on the east Australian continental shelf. Part I: Propagation of modes. *J. Phys. Oceanogr.*, **16,** 1929–1943.

——, N. J. White, A. J. Clarke, H. J. Freeland and R. L. Smith, 1986b: Coastal-trapped waves on the east Australian continental shelf. Part II: Model verification. *J. Phys. Oceanogr.*, **16,** 1945–1958.

Crawford, W. R., and R. E. Thomson, 1984: Diurnal-period continental shelf waves along Vancouver Island: A comparison of observations with theoretical models. *J. Phys. Oceanogr.*, **14,** 1629–1646.

Fandry, C. B., G. D. Hubbert and P. C. McIntosh, 1985: Comparison of predictions of a numerical model and observations of tides in Bass Strait. *Aust. J. Freshwater Res.*, **36,** 737–752.

Foreman, M. G. G., 1978: Manual for tidal current analysis and prediction. Pac. Mar. Sci. Rep., 78-6, Institute of Ocean Sciences, Sidney, B.C., Canada, 70 pp.

Freeland, H. J., F. M. Boland, J. A. Church, A. J. Clarke, A. M. G. Forbes, A. Huyer, R. L. Smith, R. O. R. Y. Thompson and N. J. White, 1986: The Australian Coastal Experiment: A search for coastal-trapped waves. *J. Phys. Oceanogr.*, **16,** 1230–1249.

Middleton, J. H., T. D. Foster and A. Foldvik, 1987: Diurnal shelf waves in the southern Weddell Sea. *J. Phys. Oceanogr.*, **17**(5), 784–791.

Thomson, R. E., and W. R. Crawford, 1982: The generation of diurnal period shelf waves by tidal currents. *J. Phys. Oceanogr.*, **12,** 635–643.

Yefimov, Y. Y., and A. B. Rabinovich, 1980: Resonant tidal currents and their relation to continental shelf waves of the northwestern Pacific Ocean. *Izv., Atmos. Oceanic Phys.*, **16**(10), 805–810.